Air Damping of Oscillating MEMS Structures: Modeling and Comparison with Experiment

Sergey Gorelick*[1], James R. Dekker[1], Mikko Leivo[1], and Uula Kantojärvi[1]

[1]VTT Technical Research Centre of Finland, Tietotie 3, Espoo, P.O.Box 1000, FI-02044 VTT, Finland
*Corresponding author: Tietotie 3, Espoo, P.O.Box 1000, FI-02044 VTT, Finland; sergey.gorelick@vtt.fi

Abstract: Air damping can be detrimental to the performance of vibrating MEMS components. Quantitative evaluation of the damping is challenging due to the complex interaction of air with moving structures and typically requires numerical simulations. A full three-dimensional analysis can be computationally very expensive, time consuming and not feasible. Here, we present a simplified two-dimensional modeling of damping per unit length of selected MEMS structures. The simulated air damping results were compared with experimental measurements of corresponding piezoactuated resonators: in-plane and out-of-plane tuning forks, two types of out-of-plane cantilevers and a torsional micromirror. The applicability of the simplified model is verified by a good (2-30%) agreement between the simulated and measured Q-values.

Keywords: MEMS, air damping, FEM, tuning fork, micromirror

1. Introduction

Various MEMS devices, resonators and sensors are designed to operate in air and viscous fluids. Excessive air damping can be detrimental to the performance of oscillating MEMS components. Quantitative evaluation of the air damping is, therefore, required already during the design stages to obtain accurate predictions of the device performance. The interaction of fluid flow with moving structures is complex such that analytical approximations of the damping coefficient are available only for simple structures and trivial boundary conditions. More complex systems with structures moving with respect to each other and in proximity to stationary objects typically require simulations to reliably evaluate the air damping. Thus, a simple out-of-plane cantilever oscillating inside a pre-etched cavity (Figure 1) experiences damping due to the interaction with several types of flow (squeeze-film, shear flow and drag due to the direct air resistance). The damping due to the individual types of flow can be evaluated using simplified analytical models [1] or circuit analysis [2,3]. However, due to the existence of intermediate flow regimes (Figure 1) and geometrical sensitivity of the fluid-structure interaction, reliable estimation of the damping coefficients requires computational flow simulations. COMSOL Multiphysics™ was previously used successfully for air damping simulations in angular comb-drive micromirrors [4]. To evaluate the applicability of the Fluid-Structure Interaction interface of COMSOL Multiphysics™ for estimation of the air damping for a variety of other MEMS devices, the experimental and simulated performance of several typical resonator MEMS systems in this paper are compared: two types of out-of-plane cantilevers, in-plane and out-of-plane tuning forks, and a torsional mirror (Figure 2). A full three-dimensional damping analysis is computationally very expensive and time-consuming. Instead, a simpler two-dimensional analysis of the damping per unit length of the structures and as a function of initial displacement was performed (Figure 2 and 3). Such an approximation neglects edge effects and, in case of a bending cantilever, also the rotary motion of the beam cross-section.

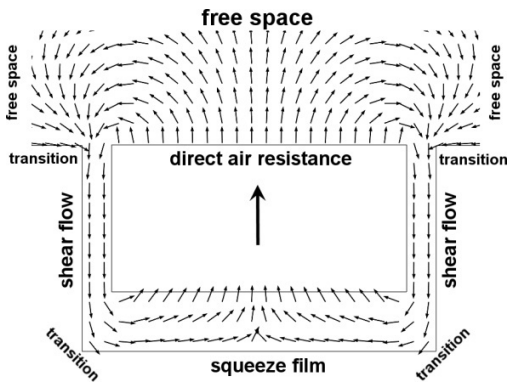

Figure 1. Air flow simulation time-snapshot of an out-of-plane cantilever oscillating inside a pre-etched cavity. The arrows indicate the velocity field of the air flow around the cross-section of the cantilever. The

arrow within the cantilever indicates instantaneous velocity of the cantilever. Several regions of flow can be identified (shear flow, squeeze-film flow, drag due to the direct air resistance) as well as transitional regions.

The validity of the approximation is, however, justified by the consistency of simulated and experimental results. The good agreement of the experimental and corresponding simulation results validate the applicability of the simplified flow model for evaluation of the air damping in other more complex system.

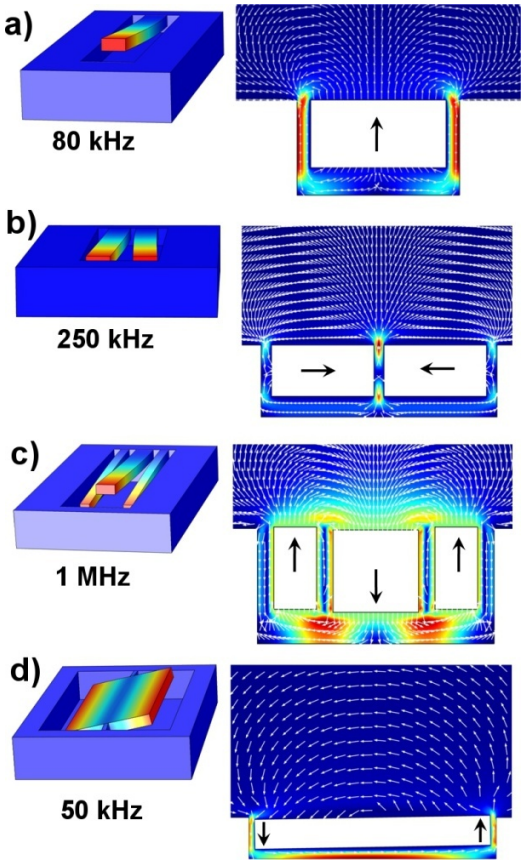

Figure 2. Simulation of air damping of various MEMS systems resonating inside pre-etched cavities using simplified two-dimensional model with numerical "springs" that replace the deformable flexures and generate restoring forces. Shown are schematic deformation of each system in 3D with the resonance frequency and corresponding simplified 2D model air flow simulation time-snapshots. a) out-of-plane cantilever, 80 kHz. b) In-plane tuning fork, 250 kHz. c) Out-of-plane tuning fork, 1 MHz. d) Torsional mirror, 50 kHz.

2. Experimental measurements

The simulated systems aimed at modeling the air damping of selected MEMS devices. The test devices, such as cantilever and torsional resonators (Fig 2), in this study were fabricated using c-SOI technology (cavity silicon on insulator) technology in 50-µm-thick device layers. The devices were actuated by means of thin (~1 µm) aluminium nitride (AlN) piezolayers processed on top of the released structures (cantilevers or actuating flexures). The air damping in the following devices was characterized experimentally:

- Wide cantilever C1 (width, height, length 100×50×900 μm^3); Resonance frequency ~80 kHz (Figure 2a).
- Narrow cantilever C2 (width, height, length 50×50×900 μm^3). Resonance frequency ~80 kHz. (not shown)
- In-plane tuning fork TF1 (width, height, length 100×50×700 μm^3). Resonance frequency ~250 kHz (Figure 2b).
- Out-of-plane tuning fork TF2 (width, height, length 26×50×238 μm^3). Resonance frequency ~1 MHz (Figure 2c).
- Torsional mirror M (width, height, length 400×50×800 μm^3). Resonance frequency ~50 kHz (Figure 2d, actuators not shown to facilitate clarity).

The characterization of the devices' performance was based on measuring their electrical admittance in a frequency range around their resonances both in vacuum and in air. The mechanical Q-values were then derived from the fits of the equivalent $R_m L_m C_m$-C_0 circuit [3,5] to the admittance-frequency curves (Figure 3). Measurement of the Q-value of the same device both in air (Q_{air}) in vacuum (Q_{vacuum}) allows isolating the damping effect due to interaction with air flow (Q_{flow}) alone from other damping effects (anchor loss, thermoelastic damping, surface losses, etc).

$$\frac{1}{Q_{air}} = \frac{1}{Q_{flow}} + \frac{1}{Q_{vacuum}} \qquad (1)$$

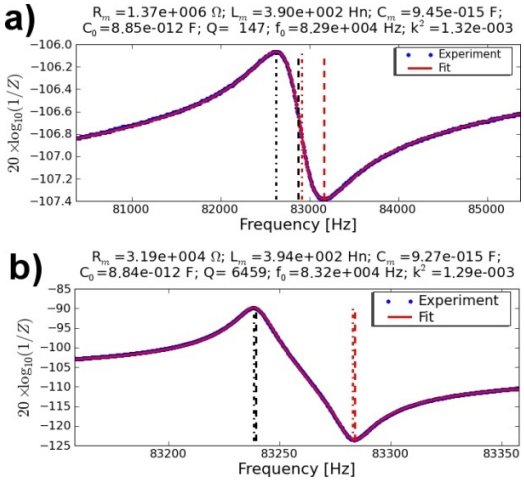

Figure 3. Measurement of electrical admittance of a piezodriven cantilever (Fig. 2a) around the resonance frequency with corresponding fits of equivalent circuit elements (a) in air with a derived Q-value of ~150, (b) in vacuum with a derived Q-value of ~6500. (Phase of the admittance not shown.)

3. Fluid flow properties and boundary conditions

Choosing the appropriate flow properties and boundary conditions is crucial for reliable estimation of the air damping. Several dimensionless quantities can be used to categorize the type of the flow. The Knudsen number (*Kn*) is defined as the the ratio of the mean free path of fluid molecules to the characteristic dimension in the system. It can be used to verify the applicability of the viscous fluid dynamics. The typical gap width in the studied system is 10-20 µm (Fig. 2c). With the mean free path of gas molecules in air at 300 K of ~70 nm, the Knudsen number equals to 3.5-7×10^{-3}. Since 10^{-3}<Kn<10^{-1}, it can be concluded that the slip flow dynamics formalism is applicable to model the air flow [6]. The stationary surfaces adjacent to the narrow gaps in the model were, therefore, defined as walls with slip boundary condition while no-slip condition was applied to further lying walls (Fig. 4c).

The Reynlods number *Re* can be used to categorize the flow as either laminar or turbulent. It is defined as

$$Re = \frac{\rho |v| L}{\mu} \qquad (2)$$

where ρ is the fluid density, v and L – characteristic velocity and dimension of the system, respectively, and μ is the dynamic viscosity of the fluid. The maximum of the Reynolds numbers for the studied systems are summarized in Table 1. With *Re*<<2000 it can be concluded that the air flow is laminar for all the studied systems and no turbulence effects needed to be included in the simulations.

device	f0 [kHz]	Q in air	Δx (AC) [µm]	v (AC) [m/s]	**Re**
C1	80	150	0.75	0.38	**0.25**
C2	80	180	0.90	0.45	**0.30**
TF1	250	1200	0.28	0.45	**0.30**
TF2	1000	5600	1.26	7.91	**5.27**
M	50	175	0.05	0.02	**0.01**

Table 1. Measured devices (C1 – wide cantilever; C2 – narrow cantilever; TF1 – in-plane tuning fork; TF2 – out-of-plane tuning fork; M – torsional resonator, micromirror. See text for further details on the devices) with simulated maximum amplitude of the tip displacement and velocity using the measured Q-values in air. The velocity can be used to estimate the Reynolds number and categorize the type of the fluid flow.

The Mach number, *M*, is defined as the ratio of the speed of structures moving through a fluid to the speed of sound in the fluid. If *M*<0.3, the gas compression effects can be neglected. From Table 1, the maximum velocities of the structures are considerably smaller than 30% of the speed of sound in air $0.3\times343\approx100$ m s^{-1}, such that the simplified incompressible flow model could be used in simulations for all the studied systems.

4. Simplified air flow model

Figure 4 depicts the principle of the simplified 2D model that replaces the more complex 3D simulation. Initially deformed beam with a tip displacement *A* (Fig. 4a) is subdivided into narrow cross-sections of width *dx* and mass *dm*, each displaced by an initial amplitude A_i, such that the combined shape of the cross-sections resembles the original beam's mode shape (Fig. 4b). The cross-sections oscillate vertically and synchronously at the resonance frequency of the original beam due to the action of spring forces *dk* (Fig 4b). Replacing a three-dimensional air

flow simulation with such a two-dimensional model is justified when the beam length is much greater than its other dimensions since the air flow profile can also be assumed to be two-dimensional. For a laminar type of flow, the interaction of different oscillating cross-sections and the air flows induced by them can be considered negligible, such that the total air damping force is a sum or an integral of viscous damping forces experienced by individual cross-sections. Modeling a cross-section of an extended torsional resonator (Fig. 2d) is appropriate due to the symmetry of the proof mass about the rotation axis along the longer dimension (neglecting the edges). In the case of a bending beam, assuming the straight motion of the cross-section is an additional approximation because the neutral axis of the beam moves not only translationally but also rotationally. For small amplitudes of vibrations of a long beam the rotational motion is, however, relatively small and can be neglected. The validity of the approximation was demonstrated in a similar approach where the tines (beams) of the tuning forks were modeled as spheres or strings of spheres in straight motion [7-12]. However, modeling rectangular cross-sections is more appropriate as they reproduce closer the original geometry of the structures.

The simulations in time domain were initiated by displacing the cross-sections of the structures by initial amplitude A from the equilibrium position (in case of torsional resonators, tilting them by angle A). Due to the restoring forces or torques, the simulated systems began to oscillate. The oscillation amplitude decayed due to the interaction with air as the simulations progressed in time, and the Q-values were estimated from the logarithmic decrement of amplitude (Fig. 4d). The restoring spring forces/torques due to the springs' deformation were replaced by numerical forces/torques. The restoring forces/torques were defined as, e.g., boundary load (Fig. 3c) $-dk(A+u)$ or $-dk(A+v)$, where dk is the spring constant per unit area (adjusted to result in the required resonance frequency of the system), and u and v are the structural displacement of the centre of mass horizontally (in-plane) and vertically (out-of-plane), respectively.

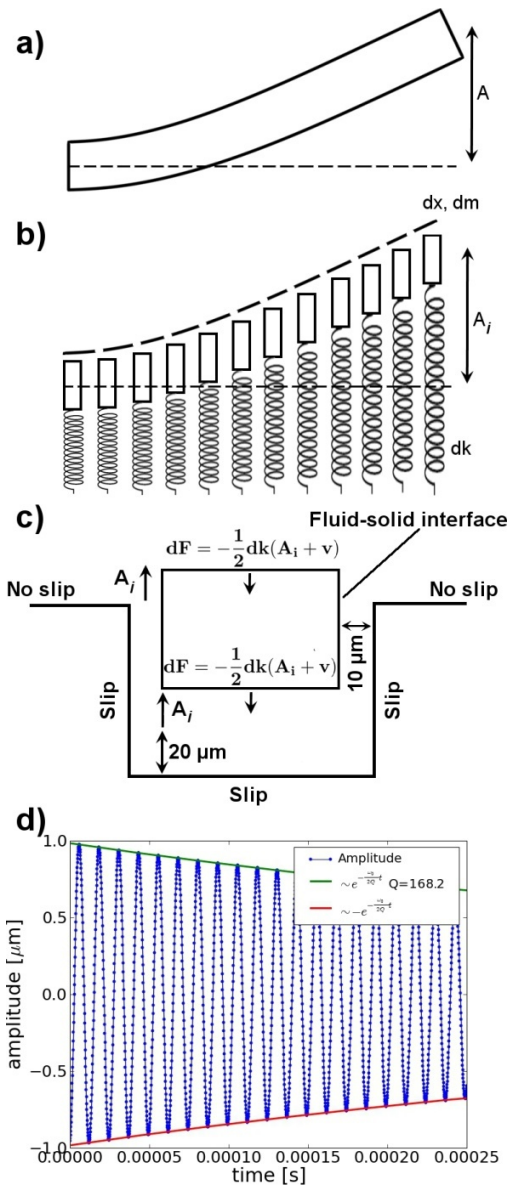

Figure 4. Schematic presentation of the simplified air damping simulation of (a) vibrating cantilever beam with an initial tip displacement A. (b) The beam is divided into cross-sections of width dx and mass dm, displaced from the equilibrium position by corresponding amplitudes A_i. The cross-sections move synchronously at the resonance frequency of the original beam due to the action of spring forces dk. (c) Cross-section of the beam inside a pre-etched cavity displaced by an initial amplitude A_i. The spring forces due to the structural deformations are replaced by boundary loads to model the restoring forces. (d) Time-domain simulation of a cantilever (Fig. 2a) cross-section displacement initially displaced by 1 µm from the equilibrium position. Due to the interaction

with air, the amplitude decays. The Q-value can be evaluated from the logarithmic decrement of the amplitude.

The numerical springs effectively replaced the action of actual restoring forces thus eliminating the need to simulate the structural deformations and reducing the simulation complexity.

5. Comparison of experimental and simulated results

Several devices of each type were characterized both in vacuum and air. The averaged Q-values derived from the electrical measurements are summarized in Table 2. The Q-values obtained in simulations are given in the same table for comparison with the experimental values. The simulated Q-values account only for losses due to the interaction of the structures with the air flow, Q_{flow}, while the Q-values measured in air, Q_{air}, include also losses due to other loss mechanisms (e.g., anchor and support losses). In order to isolate the Q-value due to the air damping alone, other contributions to the overall damping need to be filtered from the damping measured in air. These additional loss mechanisms can be estimated by performing the characterization of the devices in vacuum. Using Equation 1, the damping due to the interaction with air flow alone, Q_{flow}, can be deduced and compared directly with the corresponding simulation results (Table 2).

device	f0, kHz	Q in air	Q vacuum	**Q flow**	**Q simulated**	**Agreement**
C1	80	150	6500	**153**	**168**	**91%**
C2	80	180	6530	**185**	**265**	**70%**
TF1	250	1200	40000	**1240**	**1190**	**96%**
TF2	1000	5600	16000	**8615**	**8820**	**97%**
M	50	175	50000	**176**	**214**	**82%**

Table 2. Comparison of measured and simulated Q-values for the studied systems (C1 – wide cantilever; C2 – narrow cantilever; TF1 – in-plane tuning fork; TF2 – out-of-plane tuning fork; M – torsional resonator, micromirror. See text for further details on the devices).

The simulated Q-value were evaluated for different initial amplitudes of vibration, such that the total Q-value for a given structure could be calculated by weighing the amplitude-dependent $Q(A_i)$ with the resonant mode shape of the structure over its length. However, the simulated Q-values' variations over the typical amplitude ranges (Table 1) were insignificant.

The agreement between measured and simulated values is very good (>90%) for structures with rectangular cross-sections: wide cantilever (cross-section 100×50 µm), in-plane tuning fork (cross-section 100×50 µm), and the out-of-plane tuning fork (cross-section 26×50 µm). The agreement between the measured and simulated results is worse (70%) for the narrow cantilever with a square cross-section (50×50 µm). Even though the agreement is adequate for practical purposes, the reason for the larger mismatch is not clear. Presumably, edge effects are more pronounced in beams having square-shaped rather than rectangular cross-sections. The agreement between the measured and simulated results is relatively good (82%) for the micromirror torsional resonator with a rectangular cross-section (400×50 µm), even though the 2D model is more applicable for this type of device than for a bending beam where the rotational motion of the cross-sections is neglected. The discrepancy can be partially explained by the simplified simulation where the actuator beams were not modeled. The agreement can potentially be improved if the effects of the more complex geometry on the air flow patterns are taken into account.

The simplified 2D simulation results, however, generally fit adequately well the experimental results over a wide range of frequencies (from tens kHz to MHz) and for a variety of moving structures (in-plane, out-of-plane and torsional motion), verifying the validity of the model for estimation of the air damping in other more complex MEMS geometries and structures.

7. Conclusions

We investigated the air damping in several test MEMS piezoactuated resonating structures both experimentally and numerically. The studied test systems involved various types of motion within pre-etched cavities (in-plane, out-of-plane and torsional) and in a wide range of frequencies (10^4 – 10^6 Hz). The simplified 2D fluid-structural interaction model of the systems was used to estimate the Q-values of the studied systems that were compared with the

experimentally obtained Q-values. The simulation and experimental results generally agree very well or adequately well, with the discrepancies attributed to approximations in the model or simplifications done in the simulations. The good agreement of the simulation and experimental results validates the model and proves its feasibility for estimation of the air damping in other MEMS systems.

8. References

1. X. Zhang, W.C. Tang, Viscous air damping in laterally driven microresonators, *IEEE Workshop on Micro Electro Mechanical Systems*, **MEMS '94**, 199-204 (1994)
2. T. Veijola, T. Tinttunen, H. Nieminen, V. Ermolov, T. Ryhänen, Gas damping model for a RF MEM switch and its dynamics characteristics, *IEEE Microwave Symposium Digest*, **2**, 1213-1216 (2002)
3. V. Kaajakari, *Practical MEMS*, 184-197. Small Gear Publishing, Las Vegas (2009)
4. T. Klose, H. Conrad, T. Sandner, H. Schenk, Fluidmechanical damping analysis of resonant micromirrors with out-of-plane comb drive, *Proc. COMSOL Conf.*, **online**, http://www.comsol.com/papers/5208 (2008)
5. K.S. van Dyke, The piezo-electric resonator and its equivalent network, *Proceedings of the Institute of Radio Engineers*, **16**, 742-764 (1928)
6. S. Roy, R. Raju, Modeling gas flow through microchannels and nanpores, *Journal of Applied Physics*, **93**, 4870-4879 (2003)
7. K. Kokubun, M. Hirata, Y. Toda, M. Ono, A bending and stretching mode crystal oscillator as a friction vacuum gauge, *Vacuum*, **34**, 731-735 (1984)
8. K. Kokubun, M. Hirata, M. Ono, H. Murakami, Y. Toda, Unified formula describing the impedance dependence of a quartz oscillator on gas pressure, *J. Vac. Sci. Technol. A*, **5**, 2450-2453 (1987)
9. F.R. Blom, S. Bouwstra, M. Elwenspoek, J.H.J Fluitman, Dependence of the quality factor of micromachined silicon beam resonators on pressure and geometry, *J. Vac. Sci. Technol. B*, **10**, 19-26 (1992)
10. H. Hosaka, K. Itao, S. Kuroda, Damping characteristics of beam-shaped micro-oscillators, *Sensors and Actuators A*, **49**, 87-95 (1995)
11. H. Hosaka, K. Itao, Theoretical and experimental study on airflow damping of vibrating microcantilevers, *Joutnal of Vibration and Acoustic*, **121**, 64-69 (1999)
12. J.-H. Lee, S.-T. Lee, C.-M. Yao, W. Fang, Comments on the size effect on the microcantilever quality factor in free air space, *J. Micromech. Microeng.*, **17**, 139-146 (2007)

9. Acknowledgements

The research has been funded by Tekes (Finnish Funding Agency for Technology and Innovation), Bruco Integrated Circuits BV, Innoluce BV, SILEX Microsystems AB, VINNOVA and NL Agency (Department of International Research & Innovation), and VTT under the collaborative project of Eurostars HighResSensing. The fabrication of the samples used in this study was funded by TEKES, Murata Electronics, TDK-EPC and Okmetic under the collaborative project of PiezoMEMS. We are thankful to Diederik van Lierop and Marijn van Os from Innoluce BV, Thorbjörn Ebefors from SILEX Microsystems AB and Gerard Voshaar from Bruco Integrated Circuits BV for helpful discussions. We are also grateful to Dennis Alveringh and Sofia Lemström for help with the measurements.